Electronic Supplementary Material

Charge-carrier photogeneration and extraction dynamics of polymer solar cells probed by a transient photocurrent nearby the regime of the space charge-limited current

Boa Jin[1], Hyunmin Park[1], Yang Liu[2], Leijing Liu[2], Jongdeok An[1], Wenjing Tian[2], and Chan Im **(✉)**[1]
1 Department of Chemistry, Konkuk University, Seoul 05029, Korea
2 State Key Laboratory of Supramolecular Structure and Materials, College of Chemistry, Jilin University, Changchun 130012, China
E-mail: chanim@konkuk.ac.kr

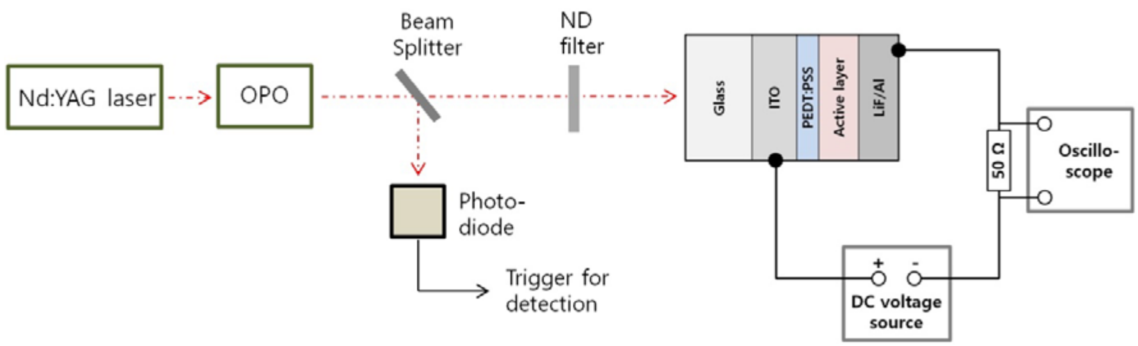

SM Fig. 1 Scheme of used TPC experimental set up with device structure.

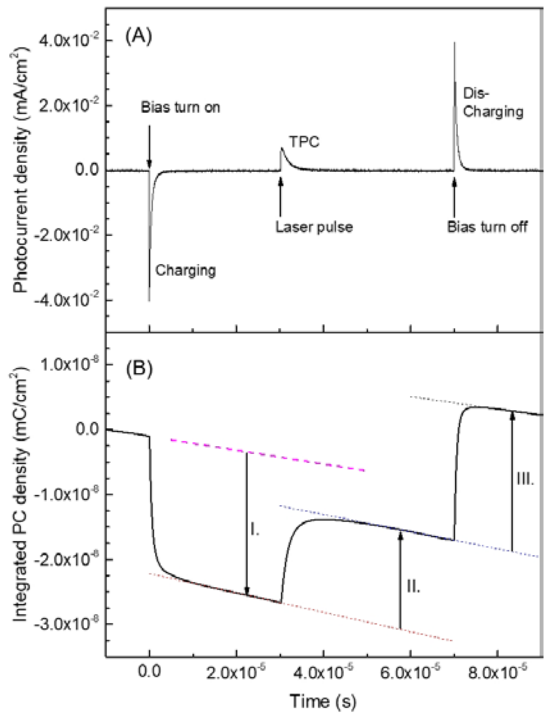

SM Fig. 2 (A) A representative trace of a TPC density with (B) a corresponding integrated TPC. I, II, and III stand for amplitudes of integrated charging, photo-, and discharging currents, respectively. This record was measured with a P3HT:PCBM solar cell.

SM Table 1 Used excitation intensities.

$T_{\text{ND filter}}$ (%)	Excitation pulse energy (J/pulse)	Photon density (photons/cm^2)	Excitation intensity (sun)
3.35×10^{-2}	6.03×10^{-9}	3.95×10^{11}	3.0×10^{2}
2.78×10^{-1}	5.01×10^{-8}	3.28×10^{12}	2.5×10^{3}
5.53×10^{-1}	9.95×10^{-8}	6.51×10^{12}	5.0×10^{3}
2.31×10^{0}	4.16×10^{-7}	2.72×10^{13}	2.1×10^{4}
4.59×10^{0}	8.26×10^{-7}	5.41×10^{13}	4.1×10^{4}
1.52×10^{1}	2.74×10^{-6}	1.79×10^{14}	1.4×10^{5}
3.02×10^{1}	5.44×10^{-6}	3.56×10^{14}	2.7×10^{5}
1.00×10^{2}	1.80×10^{-5}	1.18×10^{15}	9.0×10^{5}

In SM table 1, the incident photon densities (IPD) that were converted from the pulse energies are also listed. For convenience, the “sun” unit that is familiar to the solar-cell research community is also listed, although it is assumed that this unit was used with the AM 1.5 G solar spectrum under a continuous wave (CW) situation.

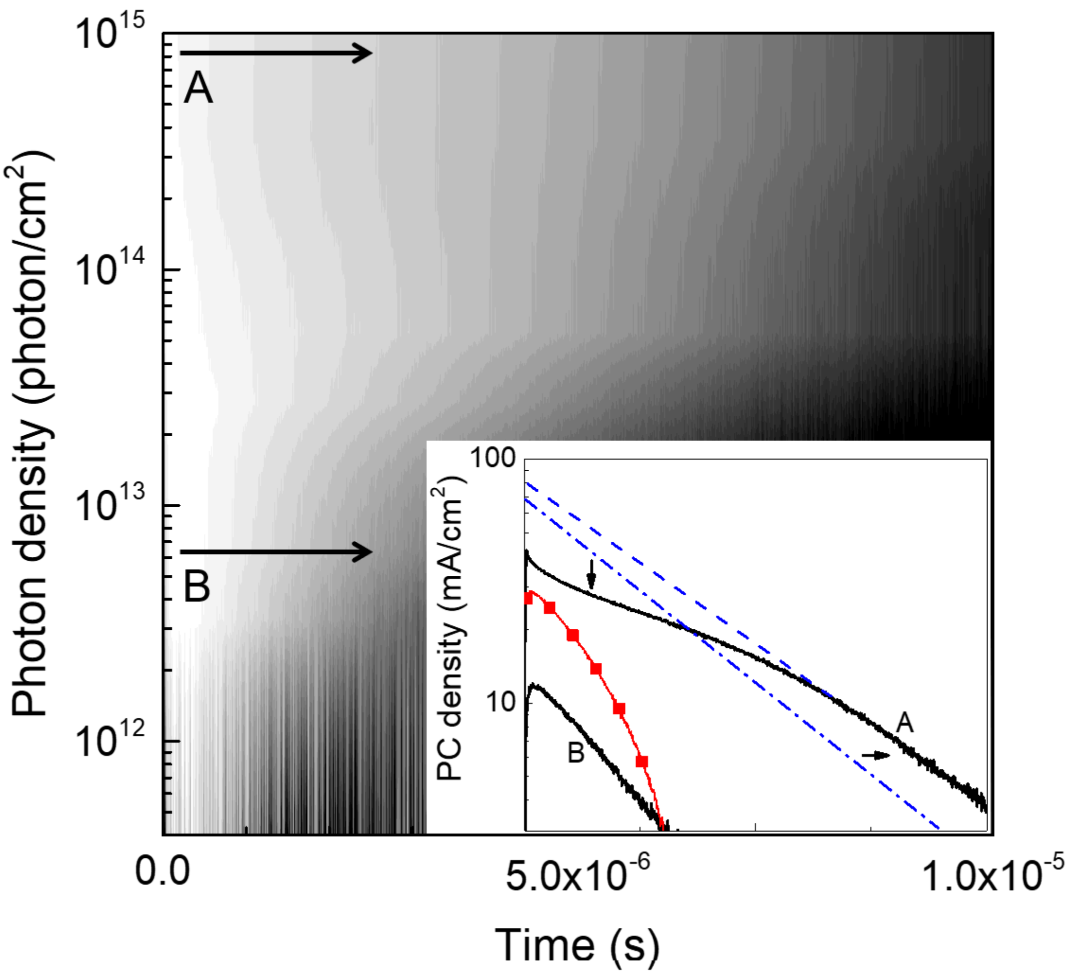

SM Fig. 3 Incident photon density (IPD)-dependent transient photocurrent (TPC)-decay map of P3HT at 0.4 V_{ext}. Inset: TPC-trace A at high IPDs and TPC-trace B at low IPDs. The map was rendered using a logarithmic gray scale according to normalized photocurrent (PC) densities, and the bright tone represents the higher PC-density values. The dash and dash-dot lines are hypothetical decays for which exponential functions were used. The curve with the rectangles is the CC-loss amount with time.

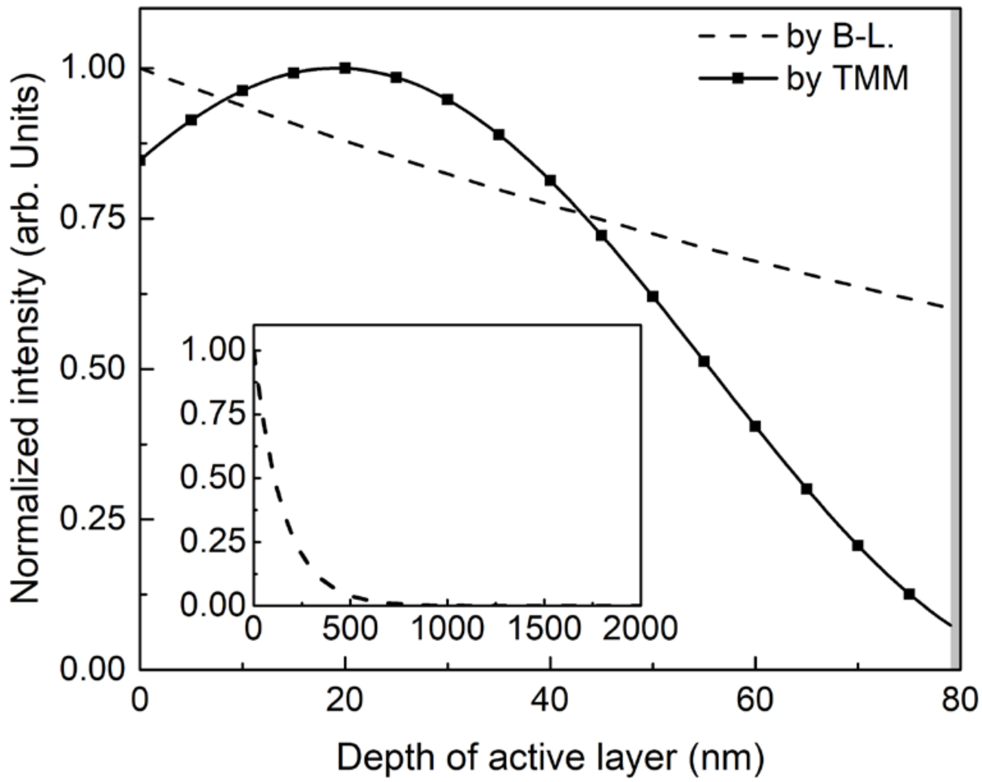

SM Fig. 4 Intensity profiles calculated using the Beer–Lambert (B–L) equation (dash line) and the transfer matrix method, or TMM (solid line with rectangles), within an active layer of a 79-nm thickness. The intensity profile that was calculated using the B-L equation with the same optical density is also shown in the inset for the 2-μm thickness.

Description for figure 9 in the manuscript

For these demonstrative maps, a set of energy values were randomly generated for a 50 × 50 matrix with a Gaussian distribution, and 20 × 20 map submatrices were chosen and are displayed to maintain an overview. The sites where the CCs can be transported to are located at each lattice position, and these sites are coloured as pixels according to their energy values that also indicate the feasibility of the visiting probability. For the classification of the energy values, quasi-equilibrium transport-energy levels were used as the critical criteria, as shown by the DOSs with the bold dash lines on the right side of the maps. Here, the effective transport energies were set as almost "-1," which is similar to the σ value of the Gaussian distribution. Further, just to show the different percolative transport channels that became apparent upon the changing of the EFs, a range of -1 ± 0.8 was given for the high EF, whereas a lower and narrower range of -1.2 ± 0.4 was given for the low EF. This demonstration also shows that CCs can more effectively overcome the potential inter-site barriers for the hopping processes at the high EF compared with those at the low EF; moreover, a further consideration of the CC situation in such a disordered system by means of a percolation under a dynamic-CC population is part of the purpose as well.